arXiv:1411.0855v1 [cond-mat.str-el] 4 Nov 2014

Low temperature crystal structure and local magnetometry for the geometrically frustrated pyrochlore $Tb_2Ti_2O_7$

P. Dalmas de Réotier[1,2], A. Yaouanc[1,2], A. Bertin[1,2], C. Marin[1,2], S. Vanishri[1,2], D. Sheptyakov[3], A. Cervellino[4], B. Roessli[3], C. Baines[5]

[1]Univ. Grenoble Alpes, INAC-SPSMS, F-38000 Grenoble, France
[2]CEA, INAC-SPSMS, F-38000 Grenoble, France
[3]Laboratory for Neutron Scattering and Imaging, Paul Scherrer Institute, CH-5232 Villigen-PSI, Switzerland
[4]Swiss Light Source, Paul Scherrer Institute, CH-5232 Villigen-PSI, Switzerland
[5]Laboratory for Muon-Spin Spectroscopy, Paul Scherrer Institute, CH-5232 Villigen-PSI, Switzerland

Abstract.

We report synchrotron radiation diffraction and muon spin rotation (μSR) measurements on the frustrated pyrochlore magnet $Tb_2Ti_2O_7$. The powder diffraction study of a crushed crystal fragment does not reveal any structural change down to 4 K. The μSR measurements performed at 20 mK on a mosaic of single crystals with an external magnetic field applied along a three-fold axis are consistent with published a.c. magnetic-susceptibility measurements at 16 mK. While an inflection point could be present around an internal field intensity slightly above 0.3 T, the data barely support the presence of a magnetization plateau.

The study of geometrically frustrated magnetic systems reveals a large variety of new magnetic phases. Among the frustrated materials, the rare-earth pyrochlore oxides which crystallize in a cubic structure ($Fd\bar{3}m$ space group) form a family for which different exotic ground states have been found [1]. Focusing on the insulators, we mention (i) the spin-ice ground state of $Ho_2Ti_2O_7$ and $Dy_2Ti_2O_7$ [2, 3], (ii) the spin-liquid ground state of $Yb_2Ti_2O_7$ [4] characterized by a pronounced peak in the specific heat for powder samples [5, 6], although an exotic ordered magnetic state has been reported for a single crystal [7, 8], (iii) the unconventional dynamical ground state of $Tb_2Sn_2O_7$ for which magnetic Bragg reflections are observed by neutron diffraction [9] while no spontaneous magnetic field is found by the zero-field positive muon spin relaxation (μSR) technique [10, 11], (iv) the persistent spin dynamics detected in the ordered states of $Gd_2Sn_2O_7$, $Gd_2Ti_2O_7$ and $Er_2Ti_2O_7$ [12, 13, 14, 15, 16], and (v) the splayed ferromagnet $Yb_2Sn_2O_7$, i.e. essentially a ferromagnetic compound [17, 18, 19], with an emergent gauge field [20].

The most mysterious compound of the rare-earth pyrochlore oxide family might be $Tb_2Ti_2O_7$ for which no long-range magnetic order is detected down to 20 mK, far below the absolute value of its Curie-Weiss temperature $\Theta_{CW} = -19$ K [21, 22]. Two theoretical ground states have been suggested: a quantum spin ice ground state proposed in Ref. [23] and a Jahn-Teller like distorted ground state based on specific heat measurements [24]. In analogy with the spin-ice systems, a magnetization plateau is expected at low temperature for an external magnetic field

$\mathbf{B}_{\rm ext}$ applied along a [111] crystal direction if the former ground state is reached [25]. While static magnetization measurements have not found any signature of the predicted plateau down to 43 mK [26, 27, 28], the presence of a weak magnetization plateau below about 0.05 K has been proposed from a.c. susceptibility experiments for $0.06 < B_{\rm ext} < 0.6$ T [29]. Pointing out to the complexity of the physics involved, an anomaly in the static magnetic response has been observed around 0.15 K [30, 22, 26, 27] which strangely enough corresponds to a minimum rather than a maximum in the specific heat [22]. Pinch points in the neutron scattering intensity have been observed [31] with dispersive excitations emerging from them [32, 33], suggesting a strong magnetoelastic coupling in the Coulomb phase of $Tb_2Ti_2O_7$. In addition, a neutron scattering intensity measured at the $\left(\frac{1}{2},\frac{1}{2},\frac{1}{2}\right)$ position in reciprocal space has attracted some attention [31, 34, 35, 36]. However, its characterization and origin are a subject of discussions.

Given the dependence of some physical properties of $Tb_2Ti_2O_7$ on the sample preparation [24, 37, 22, 6, 26, 36], here we shall first present a high-resolution synchrotron radiation diffraction study on a crushed fragment of a single crystal. Thereafter we shall report on frequency shifts as measured on a crystal by the transverse-field (TF)-μSR technique with an external field $\mathbf{B}_{\rm ext}$ applied along a three-fold axis. They give access to the thermal and field dependences of a physical quantity proportional to the static magnetization. These measurements, for which the influence of a small amount of an impurity phase, if any, should be minimum,[1] barely support the existence of magnetization plateau at 20 mK.

For the two experiments we used parts of the crystal denoted C in Refs. [24, 37, 26]. This crystal is characterized by a very small residual entropy [22], as expected for a sample in thermodynamical equilibrium [38]. We briefly recall the procedure for the crystal synthesis. A polycrystalline $Tb_2Ti_2O_7$ powder has been first prepared from commercial Tb_2O_3 and TiO_2 powders of respective purity 4N and 4N5. An initial heat treatment of these powders to 1200°C has been followed by a second treatment up to 1350°C with an intermediate grinding and compaction so as to obtain a dense rod. The crystal has been subsequently prepared from the $Tb_2Ti_2O_7$ rod using the traveling floating zone technique under oxygen gas and with a translational velocity of 7 mm/h. For the μSR measurements, plates whose normal axis is a [111] axis have been cut from the single crystal: their thickness is about 1/3 mm and their lateral size is up to 6 mm.

The synchrotron radiation measurements have been performed at the high resolution powder diffractometer of the Material Science (MS) beamline at the Swiss Light Source (Paul Scherrer Institut, Switzerland). An x-ray beam of wavelength 0.49646 Å, corresponding to an energy $\simeq$ 25.0 keV, has been used. The x-ray flux is maximum at this energy at the MS beamline [39]. A crushed fragment of the $Tb_2Ti_2O_7$ crystal and $\simeq 15$ wt.% of silicon powder have been mixed and ground to obtain a homogeneous mixture. The specimen has been loaded into a 0.3 mm diameter glass capillary. The presence of silicon helps in reducing the $Tb_2Ti_2O_7$ sample x-ray absorption and provides a convenient calibration. The data have been taken from room temperature down to 4 K.

Figure 1 displays an example of a diffraction diagram. The solid line results from a Rietveld fit. The quality of the fit is excellent. In Figs. 2 and 3 we compare the profiles of the $(12,0,0)$ and $(8,8,0)$ Bragg profiles recorded at 20 and 4 K. In contrast to the result of Ruff *et al.* [40] who found a profile broadening below 20 K, no shape change of the profiles is observed at low temperature. To further check for the behavior of our $Tb_2Ti_2O_7$ specimen, we determined the temperature dependence of the lattice parameter a. The compound exhibits the expected smooth thermal contraction as it is cooled down with a plateau below $\approx$ 25 K to $a \simeq 10.1368$ Å. In Ref. [40] an expansion was reported below 20 K. Therefore, our measurements do not support the previous claim of the presence of structural fluctuations below $\approx$ 20 K in $Tb_2Ti_2O_7$. They

[1] As an example, see A. Yaouanc *et al*, to be published.

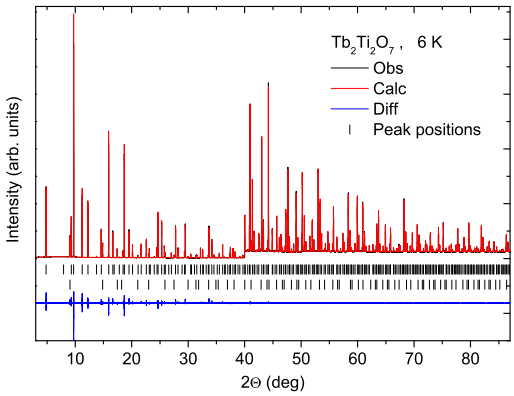

Figure 1. Rietveld refinement plot of synchrotron x-ray powder diffraction data of $Tb_2Ti_2O_7$ collected at 6 K with a photon energy of 25 keV. Observed points, calculated profile and difference curve are shown. Ticks below the graph show the calculated peak positions for $Tb_2Ti_2O_7$ and Si (upper and lower rows respectively). The intensities beyond $2\Theta = 40°$ have been enlarged by a factor of 10 in order to illustrate the agreement quality at higher angles.

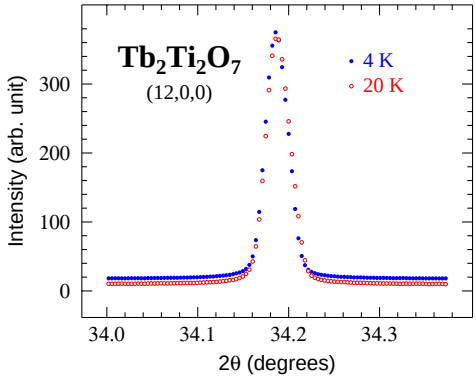

Figure 2. Comparison of the $(12, 0, 0)$ x-ray Bragg peak profiles measured at 20 and 4 K for our $Tb_2Ti_2O_7$ powder. The full width at half maximum of the Bragg peak is 9×10^{-3} in reciprocal lattice units.

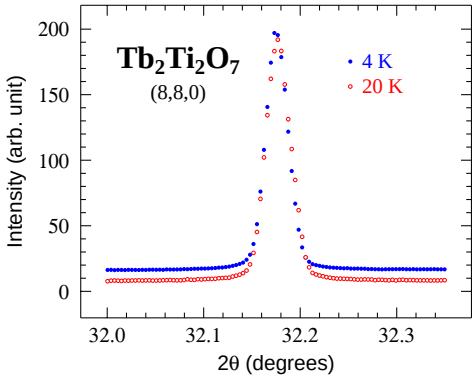

Figure 3. Comparison of the $(8, 8, 0)$ x-ray Bragg peak profiles measured at 20 and 4 K for our $Tb_2Ti_2O_7$ powder.

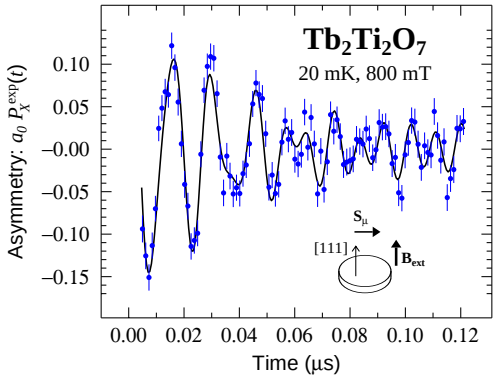

Figure 4. A typical TF-μSR asymmetry time spectrum recorded at 20 mK for a mosaic of $Tb_2Ti_2O_7$ crystals with $\mathbf{B}_{\rm ext}$ applied along a three-fold axis and $B_{\rm ext} = 800$ mT. The solid line results from a fit as explained in the main text.

are in fact fully consistent with the results of Goto *et al.* [41]. We measure for the lattice parameter $a = 10.15735\,(10)$ Å at 295 K. This is slightly larger than $a = 10.15529\,(1)$ Å recently reported [33]. In fact, as pointed out in this reference, literature values of the lattice parameter of $Tb_2Ti_2O_7$ are clustered around 10.154 Å, but outlying values do exist. This casts doubt on the assignment of composition based on the lattice parameter [36].

Finally the value for the position parameter of the oxygen ion at position $48f$ is $x = 0.32783\,(3)$

for temperatures below 50 K.[2] Above 200 K we find that it slightly decreases: $x = 0.3270\,(1)$. These values are in agreement with the literature [42].

The μSR study has been performed at the Low Temperature Facility of the Swiss Muon Source (Paul Scherrer Institute, Switzerland) with a disk made of a mosaic of crystal plates previously described. It has covered the temperature range from 20 to 500 mK. We have set $\mathbf{B}_{\rm ext}$ perpendicular to the sample disk and therefore parallel to a $Tb_2Ti_2O_7$ [111] axis, and the initial muon polarization $\mathbf{S}_\mu$ perpendicular to it. By definition $\mathbf{B}_{\rm ext}$ and $\mathbf{S}_\mu$ are parallel to the Z and X axes, respectively. The geometry of the experiment is illustrated in the inset of Fig. 4.

The quantity of interest is the TF-μSR asymmetry time spectrum $a_0 P_X^{\rm exp}(t)$, where $P_X^{\rm exp}(t)$ describes the evolution of the muon polarization under $\mathbf{B}_{\rm ext}$. The positron detectors are located perpendicular to the Z axis [43]. In Fig. 4 a typical asymmetry spectrum is displayed. It can be described as the weighted sum of two beating damped oscillating components: the first accounting for the muons implanted in the sample and the second modeling the response for the muons stopped in the sample surroundings, essentially the silver sample holder:

$$a_0 P_X^{\rm exp}(t) \;=\; a_1 \exp(-\lambda_{X,1} t)\cos(2\pi\nu_1 t + \varphi) + \; a_2 \exp(-\lambda_{X,2} t)\cos(2\pi\nu_2 t + \varphi). \qquad (1)$$

The analysis of the presented spectrum yields $a_1 = 0.192\,(13)$ and $a_2 = 0.028\,(2)$, i.e. only $\approx 13\%$ of the muons are stopped in the surroundings with $\nu_2 = 108.46\,(1)$ MHz. This latter value is very close to the precession frequency $\nu_{\rm ext} = \gamma_\mu B_{\rm ext}/(2\pi) = 108.43$ MHz expected for muons submitted to a field $B_{\rm ext} = 800$ mT. Here $\gamma_\mu = 851.6$ Mrad s^{-1} T^{-1} is the muon gyromagnetic ratio.

The interest is not in ν_1, but rather in the frequency shift $\Delta\nu = \nu_1 - \nu_2$, or more conveniently the normalized frequency shift $K_{\rm exp} = \Delta\nu/\nu_2$ which, to a good approximation, can be written as $K_{\rm exp} = \Delta\nu/\nu_{\rm ext}$. This quantity, already known to be negative for $Tb_2Ti_2O_7$ [44, 22], is displayed in Fig. 5 versus $B_{\rm ext}$ for $T = 500$ and 20 mK. Relative to the data at 500 mK, at 20 mK an extra contribution to $K_{\rm exp}$ appears below ≈ 0.6 T. This is consistent with the first magnetization curves recorded at 500 and 57 mK which also differentiate themselves only below 0.5 T [26]. Following the difficulties recently pointed out to correct for demagnetization [45], we shall refrain to do it for our data. However, the qualitative consistency of our data and the magnetizations displayed in Ref. [26], for which demagnetization corrections were not required, suggests our field scale to be correct.

Since $Tb_2Ti_2O_7$ is an insulator, only the dipole field from the terbium magnetic moments contributes to the frequency shift. For the sake of derivation, assuming the sample to be a sphere, i.e. the relevant demagnetization coefficient $N^Z = 1/3$, $K_{\rm exp} = K'_{\rm dip} = \mathcal{D}^{ZZ}(\mu_0 M/B_{\rm ext})$ where $K'_{\rm dip}$ accounts for the shift from the dipole field arising from the magnetic moments inside the Lorentz sphere, $\mathcal{D}^{ZZ}$ is a dipole tensor element, and M is the magnetization along a three-fold axis. Note that if we were in the linear regime of the magnetization, the term in parentheses would be the magnetic susceptibility χ and we would recover the usual formula [43] $K_{\rm exp} = K'_{\rm dip} = \mathcal{D}^{ZZ}\chi$.[3] Hence, we expect the product $-B_{\rm ext}K_{\rm exp}$ to be proportional to M. In Fig. 6 we plot this product versus $B_{\rm ext}$. If there was a definitive plateau in the magnetization, the product would be field independent in a finite field range. This is not observed. However, as indicated by the up-arrow, a weak inflection point is present for the 20 mK data at $B_{\rm ext} \simeq 0.66$ T. It has disappeared at 500 mK.

Yin *et al.* have performed a.c. magnetic-susceptibility measurements for a $Tb_2Ti_2O_7$ crystal [29] with $\mathbf{B_{ext}}$ parallel to a three-fold axis. The data presented in their Fig. 1d for $T = 16$ mT have been recorded with an a.c. field amplitude of 0.94 mT and $B_{\rm ext}$ extending up to 1.5 T.

[2] The x values are given for the description of the space group with the origin at site of symmetry $.\overline{3}m$. The origin of the lattice is occupied by a titanium atom.

[3] Here we have neglected the anisotropy of the susceptibility.

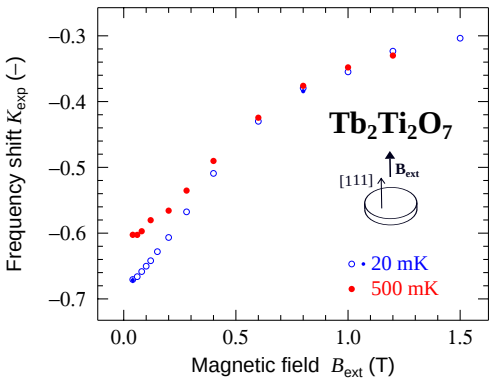

Figure 5. Field intensity dependence of the normalized frequency shift $K_{\rm exp}$ for our mosaic of $Tb_2Ti_2O_7$ crystals. $\mathbf{B}_{\rm ext}$ has been applied along a three-fold axis. The shifts have been measured at 20 and 500 mK. The error bars are smaller than the symbols. The data at 20 mK shown by open circles have been measured after zero-field cooling by increasing $B_{\rm ext}$ up to 1.5 T. Further data (small bullets) recorded after decreasing $B_{\rm ext}$ to 800 and 40 mT show no hysteretic effect. In contrast, an hysteretic response at 60 mT and low temperature has been observed in a temperature scan [22].

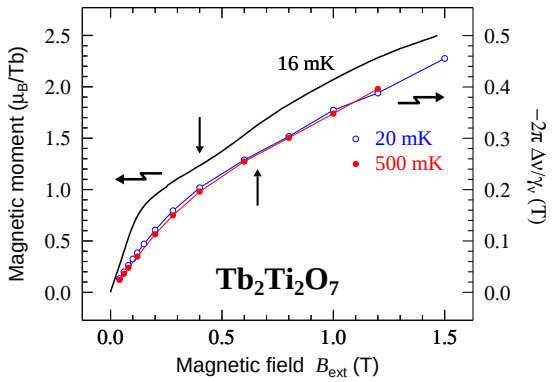

Figure 6. Open circles and bullets: product $-B_{\rm ext}K_{\rm exp} = -2\pi\Delta\nu/\gamma_\mu$ deduced from the 20 and 500 mK data displayed in Fig. 5, versus $B_{\rm ext}$. The experimental points are linked by segments. Solid line: field dependence of the terbium magnetic moment measured at 16 mK for $\mathbf{B}_{\rm ext}$ applied along a [111] crystal direction. As explained in the main text, the latter curve is computed from the data published by Yin *et al* [29].

With these experimental conditions the measurements give access to $\mu_0 {\rm d}\chi'_Z/{\rm d}B_{\rm ext}$ rather than χ'_Z, where χ'_Z is the real part of the susceptibility. This means that M can be deduced from the data of Yin *et al.* by field integration. Normalizing the result by the volume per terbium ion and dividing by the electronic Bohr magneton, we obtain the magnetic moment per terbium ion versus $B_{\rm ext}$ displayed in Fig. 6. An inflection point occurs at $B_{\rm ext} \simeq 0.40$ T as indicated by the down-arrow. In Fig. 1d of Ref. [29] the data were not corrected for the demagnetization field. However, it is relatively small: about 60 mT around 0.6 T; see Note 35 in Ref. [29]. Because of our experimental geometry, see Fig. 5, it is expected to be larger in our case. Assuming a reasonable demagnetization field of ≈ 0.30 T at 0.66 T, the position of the inflection point inferred from our data and from Ref. [29] would coincide. Expressed in terms of the internal magnetic field, the inflection point would be located slightly above 0.3 T.

Therefore our μSR measurements and a.c. susceptibility data suggest an inflection point in the magnetization could be present slightly above 0.3 T at low temperature. As deduced from Fig. 6, there is an apparent discrepancy between the two data sets at lower field. However, since the initial slope of the magnetization curve at 57 mT is about $10\,\mu_{\rm B}$/T [26], we compute a susceptibility of ≈ 1.8, a quite large value, in agreement with the literature [29]. Our frequency shift data at low field are therefore mainly controlled by the shape of our mosaic sample. From Ref. [26] we estimate $\mu_0 M/B_{\rm ext}$ to be about three times smaller at 0.4 T. This much smaller value explains that the field dependence of the two data sets are similar at high field.

The authors of the a.c. susceptibility measurements have stressed that χ'_Z displays a bump at $B_{\rm ext} \simeq 0.5$ T for $T = 40$ mK only if the field is swept sufficiently slowly, i.e for 0.625 mT/min but not for 3.75 mT/min; see Fig. S2 of the supplemental material to Ref. [29]. Our measurement

sequences have consisted of changing $B_{\rm ext}$ step by step, taking between 10 to 20 min for a field change. This is therefore quicker than 0.625 mT/min. However, when at a given $B_{\rm ext}$ value, we stood there without any field change about 1 hour for data taking. This is in contrast to the a.c. susceptibility measurements done with an a.c. field of frequency 9.6 Hz for the data of Fig. S2 and 0.21 Hz for the measurements presented in Fig. 1d.

In summary, we have reported a high resolution synchrotron radiation diffraction investigation of a piece of a crushed $Tb_2Ti_2O_7$ single crystal, and frequency shift μSR measurements at 20 mK on a mosaic of single crystals of the same compound for an external field applied along a three-fold axis. The x-ray study has not revealed any structure change down to 4 K, confirming the high quality of our crystals. The μSR measurements have given us access to a quantity proportional to the terbium magnetic moment. While an inflection point seems to be present slightly above 0.3 T for the field dependence of the moment at the lowest temperature, in agreement with previously published a.c. susceptibility data, there is barely any signature of a magnetization plateau.

Acknowledgments

PDR gratefully acknowledges partial support of Prof. H. Keller from the University of Zurich for the μSR measurements. Part of this work has been performed at the Swiss Light Source and the Swiss Muon Source, Paul Scherrer Institute, Villigen, Switzerland.

References

[1] Gardner J S, Gingras M J P and Greedan J E 2010 *Rev. Mod. Phys.* **82** 53
[2] Harris M J, Bramwell S T, McMorrow D F, Zeiske T and Godfrey K W 1997 *Phys. Rev. Lett.* **79** 2554–2557
[3] Ramirez A P, Hayashi A, Cava R J, Siddharthan R and Shastry B S 1999 *Nature* **399** 333
[4] Hodges J A, Bonville P, Forget A, Yaouanc A, Dalmas de Réotier P, André G, Rams M, Królas K, Ritter C, Gubbens P C M, Kaiser C T, King P J C and Baines C 2002 *Phys. Rev. Lett.* **88** 077204
[5] Yaouanc A, Dalmas de Réotier P, Marin C and Glazkov V 2011 *Phys. Rev. B* **84** 172408
[6] Ross K A, Yaraskavitch L R, Laver M, Gardner J S, Quilliam J A, Meng S, Kycia J B, Singh D K, Proffen T, Dabkowska H A and Gaulin B D 2011 *Phys. Rev. B* **84** 174442
[7] Yasui Y, Kanada M, Ito M, Harashina H, Sato M, Okumura H, Kakurai K and Kadowaki H 2002 *J. Phys. Soc. Jpn.* **71** 599
[8] Chang L J, Onoda S, Su Y, Kao Y J, Tsuei K D, Yasui Y, Kakurai K and Lees M R 2012 *Nat. Commun.* **3** 992
[9] Mirebeau I, Apetrei A, Rodríguez-Carvajal J, Bonville P, Forget A, Colson D, Glazkov V, Sanchez J P, Isnard O and Suard E 2005 *Phys. Rev. Lett.* **94** 246402
[10] Dalmas de Réotier P, Yaouanc A, Keller L, Cervellino A, Roessli B, Baines C, Forget A, Vaju C, Gubbens P C M, Amato A and King P J C 2006 *Phys. Rev. Lett.* **96** 127202
[11] Bert F, Mendels P, Olariu A, Blanchard N, Collin G, Amato A, Baines C and Hillier A D 2006 *Phys. Rev. Lett.* **97** 117203
[12] Bertin E, Bonville P, Bouchaud J P, Hodges J A, Sanchez J P and Vulliet P 2002 *Eur. Phys. J. B* **27** 347–354
[13] Yaouanc A, P Dalmas de Réotier, Glazkov V, Marin C, Bonville P, Hodges J A, Gubbens P C M, Sakarya S and Baines C 2005 *Phys. Rev. Lett.* **95** 047203
[14] Chapuis Y, Dalmas de Réotier P, Marin C, Yaouanc A, Forget A, Amato A and Baines C 2009 *Physica B* **404** 686
[15] Lago J, Lancaster T, Blundell S J, Bramwell S T, Pratt F L, Shirai M and Baines C 2005 *J. Phys.: Condens. Matter* **17** 979
[16] Dalmas de Réotier P, Yaouanc A, Chapuis Y, Curnoe S H, Grenier B, Ressouche E, Marin C, Lago J, Baines C and Giblin S R 2012 *Phys. Rev. B* **86** 104424
[17] Yaouanc A, Dalmas de Réotier P, Bonville P, Hodges J A, Glazkov V, Keller L, Sikolenko V, Bartkowiak M, Amato A, Baines C, King P J C, Gubbens P C M and Forget A 2013 *Phys. Rev. Lett.* **110** 127207
[18] Dun Z L, Choi E S, Zhou H D, Hallas A M, Silverstein H J, Qiu Y, Copley J R D, Gardner J S and Wiebe C R 2013 *Phys. Rev. B* **87** 134408
[19] Lago J, Živković I, Piatek J O, Álvarez P, Hüvonen D, Pratt F L, Díaz M and Rojo T 2014 *Phys. Rev. B* **89** 024421
[20] Savary L and Balents L 2012 *Phys. Rev. Lett.* **108** 037202

[21] Gardner J S, Dunsiger S R, Gaulin B D, Gingras M J P, Greedan J E, Kiefl R F, Lumsden M D, MacFarlane W A, Raju N P, Sonier J E, Swainson I and Tun Z 1999 *Phys. Rev. Lett.* **82** 1012–1015
[22] Yaouanc A, Dalmas de Réotier P, Chapuis Y, Marin C, Vanishri S, Aoki D, Fåk B, Regnault L P, Buisson C, Amato A, Baines C and Hillier A D 2011 *Phys. Rev. B* **84** 184403
[23] Molavian H R, Gingras M J P and Canals B 2007 *Phys. Rev. Lett.* **98** 157204
[24] Chapuis Y, Yaouanc A, Dalmas de Réotier P, Marin C, Vanishri S, Curnoe S H, Vâju C and Forget A 2010 *Phys. Rev. B* **82** 100402(R)
[25] Molavian H R and Gingras M J P 2009 *J. Phys.: Condens. Matter* **21** 172201
[26] Lhotel E, Paulsen C, Dalmas de Réotier P, Yaouanc A, Marin C and Vanishri S 2012 *Phys. Rev. B* **86** 020410(R)
[27] Legl S, Krey C, Dunsiger S R, Dabkowska H A, Rodriguez J A, Luke G M and Pfleiderer C 2012 *Phys. Rev. Lett.* **109** 047201
[28] Sazonov A P, Gukasov A, Cao H B, Bonville P, Ressouche E, Decorse C and Mirebeau I 2013 *Phys. Rev. B* **88** 184428
[29] Yin L, Xia J S, Takano Y, Sullivan N S, Li Q J and Sun X F 2013 *Phys. Rev. Lett.* **110** 137201
[30] Luo G, Hess S T and Corruccini L R 2001 *Phys. Lett. A* **291** 306–310
[31] Fennell T, Kenzelmann M, Roessli B, Haas M K and Cava R J 2012 *Phys. Rev. Lett.* **109** 017201
[32] Guitteny S, Robert J, Bonville P, Ollivier J, Decorse C, Steffens P, Boehm M, Mutka H, Mirebeau I and Petit S 2013 *Phys. Rev. Lett.* **111** 087201
[33] Fennell T, Kenzelmann M, Roessli B, Mutka H, Ollivier J, Ruminy M, Stuhr U, Zaharko O, Bovo L, Cervellino A, Haas M K and Cava R J 2014 *Phys. Rev. Lett.* **112** 017203
[34] Petit S, Bonville P, Robert J, Decorse C and Mirebeau I 2012 *Phys. Rev. B* **86** 174403
[35] Fritsch K, Ross K A, Qiu Y, Copley J R D, Guidi T, Bewley R I, Dabkowska H A and Gaulin B D 2013 *Phys. Rev. B* **87** 094410
[36] Taniguchi T, Kadowaki H, Takatsu H, Fåk B, Ollivier J, Yamazaki T, Sato T J, Yoshizawa H, Shimura Y, Sakakibara T, Hong T, Goto K, Yaraskavitch L R and Kycia J B 2013 *Phys. Rev. B* **87** 060408
[37] Chapuis Y 2009 *Frustration géométrique, transitions de phase et ordre dynamique* Ph.D. thesis Université Joseph Fourier Grenoble
[38] Revell H M, Yaraskavitch L R, Mason J D, Ross K A, Noad H M L, Dabkowska H A, Gaulin B D, Henelius P and Kycia J B 2013 *Nature Phys.* **9** 34
[39] Willmott P R, Meister D, Leake S J, Lange M, Bergamaschi A, Böge M, Calvi M, Cancellieri C, Casati N, Cervellino A, Chen Q, David C, Flechsig U, Gozzo F, Henrich B, Jäggi-Spielmann S, Jakob B, Kalichava I, Karvinen P, Krempasky J, Lüdeke A, Lüscher R, Maag S, Quitmann C, Reinle-Schmitt M L, Schmidt T, Schmitt B, Streun A, Vartiainen I, Vitins M, Wang X and Wullschlegera R 2013 *J. Synchrotron Rad.* **20** 667–682
[40] Ruff J P C, Gaulin B D, Castellan J P, Rule K C, Clancy J P, Rodriguez J and Dabkowska H A 2007 *Phys. Rev. Lett.* **99** 237202
[41] Goto K, Takatsu H, Taniguchi T and Kadowaki H 2012 *J. Phys. Soc. Jpn* **81** 015001
[42] Helean K B, Ushakov S V, Brown C E, Navrotsky A, Lian J, Ewing R C, Farmer J M and Boatner L A 2004 *J. Solid State Chem.* **177** 1858
[43] Yaouanc A and Dalmas de Réotier P 2011 *Muon Spin Rotation, Relaxation, and Resonance: Applications to Condensed Matter* International Series of Monographs on Physiscs 147 (Oxford: Oxford University Press)
[44] Ofer O, Keren A and Baines C 2007 *J. Phys.: Condens. Matter* **19** 145270
[45] Bovo L, Jaubert L D C, Holdsworth P C W and Bramwell S T 2013 *J. Phys.: Condens. Matter* **25** 386002